ACS APPLIED MATERIALS & INTERFACES

Research Article

www.acsami.org

Repetitive Cleavage of Elastomeric Membrane via Controlled Interfacial Fracture

Jeong Hun Kim,[†,‡] Yong Whan Choi,[†,‡] Min Sung Kim,[†] Hyung Sik Um,[†] Sung Hoon Lee,[†] Pilnam Kim,*[,§] and Kahp-Yang Suh[†,‡]

[†]School of Mechanical and Aerospace Engineering, and [‡]Division of WCU Multiscale Mechanical Design, School of Mechanical and Aerospace Engineering, Seoul National University, Seoul 151-742, Korea

[§]Department of Bio and Brain Engineering, KAIST, Daejeon 305-701, Korea

Supporting Information

ABSTRACT: Here, we report a method of fabricating thin layer of polydimethylsiloxane (PDMS), with a thickness in the range of 60−80 nm, which can be repeatedly generated (more than 10 times) from the same block of PDMS via controlled interfacial fracture. The thin layers can be transferred to various substrates by peeling off from the bulk PDMS. The cleavage is attributed to the built-in stress at the fracture interface due to plasma treatment, resulting in the repetitive formation of the thin membranes, with no residue from processing, and with a surface roughness of ∼5 nm. We were able to demonstrate transferred patterns with controlled thickness by varying the oxygen plasma treatment conditions and the composition of bulk PDMS stamp. Using the method, we achieved residual-free patterns with submicrometer resolution for applications in biomolecule array templates.

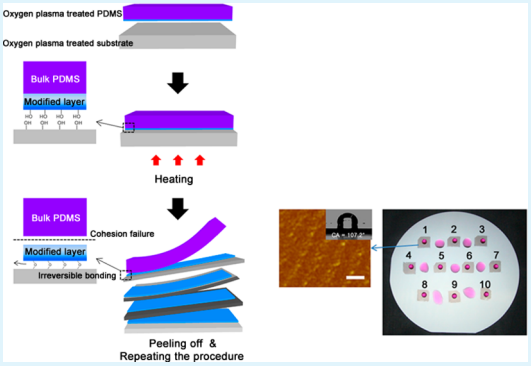

KEYWORDS: *interfacial fracture, elastic mismatch, decal transfer, polymer patterning, nano membrane*

1. INTRODUCTION

Elastic and deformable materials are used widely in applications including micro-/nanofabrication and functional structures.[1−3] A broad range of physical and chemical properties, including the elastic modulus, strength, optical properties, and surface characteristics, can be controlled and adapted to specific purposes by varying the curing conditions and chemical composition, complex mixture, and physical treatment (i.e., UV radiation and plasma treatment).[4−7] Furthermore, rubber-like materials can be used as compliant substrates to form bilayer structures with a rigid film by depositing additional layers or chemically modifying surfaces.[8−11]

A thin membrane of an elastic material has a number of advantages, including flexibility, transparency, permeability, and the ability to make conformal contact with other materials. There have been a number of reports of the fabrication of mechanically robust and functional thin membranes using spin coating, spray coating, and electrochemical synthesis, and such ultrathin membranes have applications as gas barriers, chemical sensors, and in selective extraction of the metal ions.[12−16] In addition, fabrication of advanced membranes via micro-/nanopatterning or designing composite structure may be feasible.

In this Article, we describe a simple and reproducible method of preparing thin membranes that can be repeatedly separated from pristine polydimethylsiloxane (PDMS), with a uniform thickness of 60−80 nm. By exploiting tight bonding, combined with heating and oxygen plasma treatment, subsequent cleavage via controlled interfacial fracture can be achieved. PDMS was treated with a plasma or ultraviolet (UV)-generated ozone. Because the modified layer has a large built-in stress and mechanical and chemical properties different from those of pristine bulk PDMS,[17,18] failure can occur during a contact-based transfer process. In this way, various micro-/nanoscale patterns can be generated on receiver substrates including glass, silicon dioxide (SiO_2), and flexible polymers. A number of modified decal transfer lithography (DTL) methods, based on annealing- or solvent swelling-induced cohesive mechanical failure (CMF) processes, have been reported.[19−23]

The process described here could be repeated more than 10 times without appreciable variation in properties of the transferred layers. As we shall show, varying the experimental conditions allows us to control the location of the fracture plane, and hence the thickness of the transferred layer. The surface oxidation could be controlled by varying the treatment time and plasma power, and was affected by the cross-linking density, which could be modified in a number of ways, including by changing the amount of curing agent, the baking time, and the temperature.[24−27] The thickness of transferred membrane could be controlled by varying the process

Received: April 24, 2014
Accepted: July 2, 2014
Published: July 2, 2014

conditions, because the location of the interfacial failure plane depends on the plasma treatment conditions and the cross-linking density in the PDMS. Various micro- and nanostructures could be fabricated without a residual layer by combining controlled interfacial fracture and pattern transfer methods. Because the substrate and transferred layer have different wettabilities, we were able to demonstrate the use of well-defined protein arrays for immunoassay applications.

2. EXPERIMENTAL DETAILS

Fabrication of PDMS Stamp. The silicon masters having line pattern were prepared by conventional photolithography and etching processes. The line pattern had 800 nm width with equal spacing. Its height was 600 nm, and the patterned field was 3 × 3 cm. To prepare PDMS replicas, the base and curing agent of Sylgard 184 (Dow Corning) were mixed at 10:1 wt % fraction, poured onto the silicon masters, and cured at 70 °C for various baking times (0.5−48 h). The cured PDMS stamps then were peeled from the silicon masters and cut prior to use.

Repetitive Transfer by Interfacial Fracture. The prepared PDMS stamp and substrates (bare silicon wafer, glass, or PET film) were treated by oxygen plasma under various conditions (200 mTorr, 7−18 W) for the duration from 30 s to 1 min. The stamp then was uniformly placed on the substrate, and heated on a hot plate for 20 s at 100 °C. Subsequently the stamp was peeled off from the substrate, leaving behind a thin PDMS layer on the receiver substrate. Especially, the PET film was spin coated with adhesion primer (Minuta technology, KOREA).

Atomic Force Microscopy (AFM) and Scanning Electron Microscopy (SEM). The heights of transferred membranes and patterns were measured by AFM (XE-150, psia) via noncontact mode (NCHR probe, radius of curvature <10 nm) with the scan rate of 0.5 Hz, and SEM (S-48000, Hitachi, Japan) with a Pt layer of 30 nm thickness to avoid charging effect. The emitted energy was 10 kV with 1 nm resolution.

Auger Electron Spectroscopy (AES). The elemental contents of a transferred membrane of ∼80 nm thickness were analyzed with AES (PHI-660, PerkinElmer) to measure depth profiles of three major elements (C, O, Si).

Fourier Transform Infrared (FTIR) Spectrophotometer. FTIR spectrophotometer results were recorded on a Nicolet 6700, in the mid range from 4000 to 600 cm^{-1} with 1 cm^{-1} resolution at room temperature (about 22 ± 1 °C). Both pristine PDMS membrane and transferred membrane were measured in absorbance mode, and the Ge crystal was used to measure thin layer (<300 nm) in the FTIR analysis.

Protein Immobilization and Immunostaining. For protein immobilization, human fibronectin (HFN) was used as a representative protein. Prepared samples were covered with HFN solution (5 μg/mL, Sigma) and incubated for 30 min at room temperature. After the immobilization process, samples were washed with PBST (0.1% Triton X-100 (Sigma) in PBS solution) three times to remove unbound HFN and treated with blocking solution (2% bovine serum albumin (BSA, Sigma) in PBST) for 30 min to reduce nonspecific binding of antibodies. Rabbit antifibronectin antibody solution (1:250 in blocking solution, Sigma), primary antibody solution, was pipetted onto fibronectin-immobilized samples and incubated for 1 h at room temperature. After being washed with PBST three times, fluorescein isotiocyanate (FITC) conjugated goat antirabbit IgG (1:250 in blocking solution, Sigma), secondary antibody solution, was pipetted onto samples, incubated for 1 h at room temperature in darkness, and washed three times with PBST. To prevent photobleaching of the dye, samples were coated with ProLong Gold antifade reagent (Invitrogen) and observed with florescence microscopy (Eclipse Ti, Nikon).

3. RESULTS AND DISCUSSION

We were able to achieve repeatability of the location of the failure plane at the interface of the plasma treated layer and the bulk pristine PDMS, which results in a clean interface between the layers, and a controlled thickness of the transferred membrane. In the presence of an external force, or residual stress, fracture typically occurs at the interface of a bilayer system due to the large mismatch in elasticity, so that cleavage is initiated due to a spatial gradient of the stress.[28] Because of this mismatch in the elasticity, CMF can be exploited to create micro- and nanostructures.[29] When a peeling force is applied to the bilayer system, the peeling stress is concentrated at the interface due to the mismatch in the mechanical properties of the materials.[28] The combined process of heating and peeling was able to induce clean cleavage of the oxidized PDMS layer onto various substrates, including silicon, aluminum, stainless steel, and polymer (see Supporting Information Figure S1).

The experimental procedure is illustrated in Scheme 1. A bulk PDMS block and a receiver substrate (silicon, glass, or PET film) were subjected to oxygen plasma treatment, and then placed in direct contact, followed by a short period of heat treatment (20 s at 100 °C). Following removal of the PDMS block, a thin silica-like oxidized layer was transferred to the substrate. The thickness of this layer was in the range 60−80 nm. It is well-known that oxygen plasma treatment can introduce hydrophilic silanol (−OH) groups onto the surfaces such as silicon, glass, and polymers.[30] These polar groups lead to an irreversible seal by dehydration via the following chemical reaction: SiOH + SiOH → Si−O−Si + H_2O.[31] The modified PDMS surface was much stiffer that the bulk PDMS, and had a lower thermal expansion coefficient due to the significant insertion of oxygen networks (i.e., siloxane bonds). The penetration depth of siloxane bonds is typically ∼80 nm following oxygen plasma treatment,[32] and the elastic modulus of the modified skin layer was 3−4 orders of magnitude larger than that of bulk PDMS.[33,34] This large mismatch in elasticity, in combination with the irreversible bonding at the surface, results in cohesion failure during peeling.

Scheme 1. Schematic Illustrations for Cohesion Failure of PDMS Block

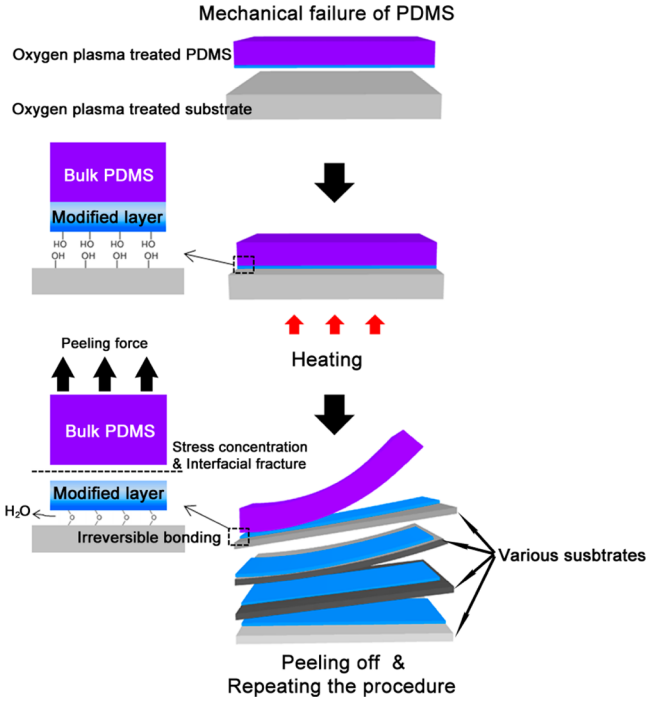

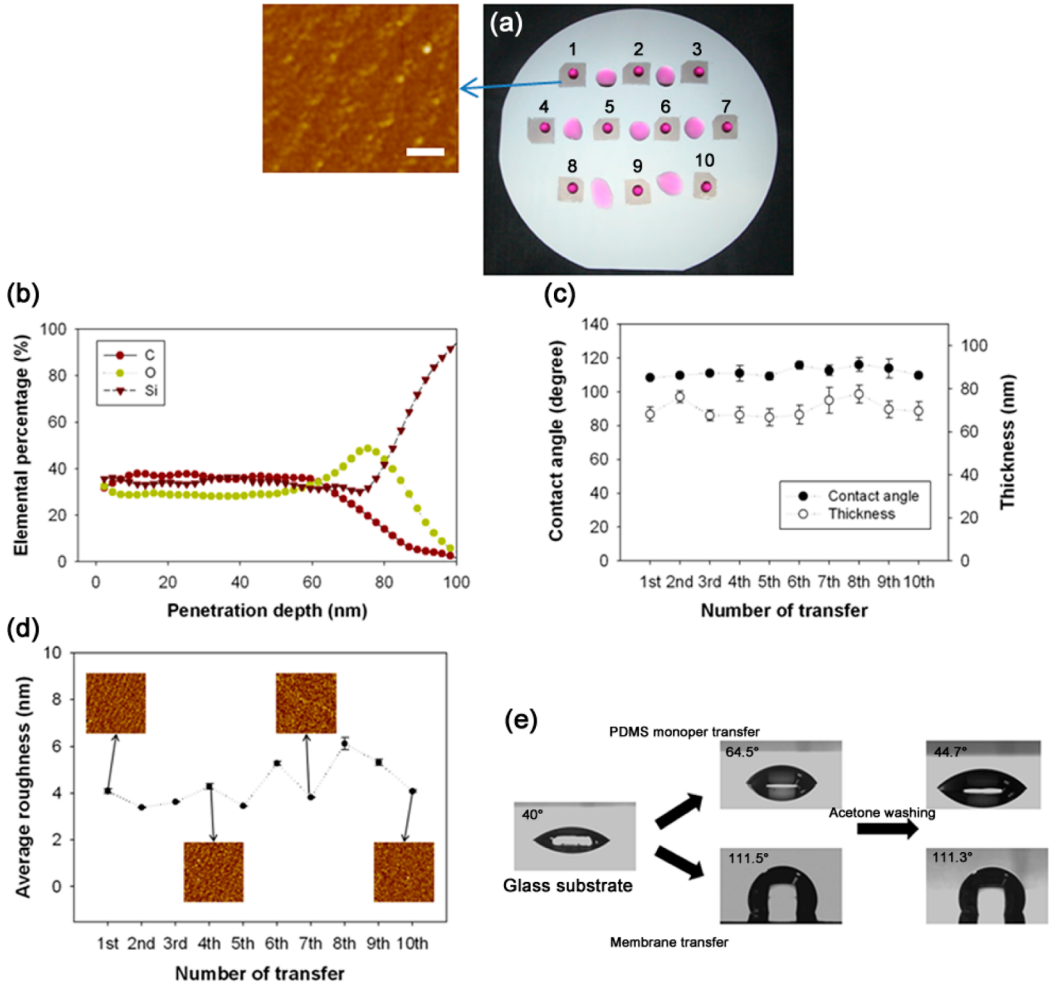

Figure 1. (a) The digital camera image of the membrane repetitively transferred to 10 times from same PDMS stamp and its AFM image. Scale bar represents 2 μm. (b) Relative elemental content of C, O, Si of the membrane along depth profile. (c) CA and height of the membranes repetitively transferred from same PDMS stamp. (d) Average roughness of repetitively transferred membranes. Area of AFM image is 10 μm^2. (e) Contact angle comparison result of PDMS oligomer and membrane transferred glass substrate.

Repetitive Transfer of the Modified PDMS Membrane. We were able to transfer the modified PDMS membranes from the same PDMS block onto 4-in. silicon wafers more than 10 times. Furthermore, uniform properties of the transferred layer were achieved, as shown in Figure 1a. The transferred region was hydrophobic with a contact angle (CA) for water of 110°, whereas the silicon wafer exhibited a CA of 20°. The CA was similar to that of the pristine PDMS, suggesting that the transferred membrane exhibited a silica-like skin layer, and an unmodified PDMS layer at the fracture surface. Depth profiles of the C, O, and Si fraction based on Auger electron spectroscopy (AES) measurement are shown in Figure 1b: the element composition was approximately 40% C, 30% O, and 30% Si, at the fracture interface, and this composition was maintained for approximately 50 nm into the thin layer. This composition deviates slightly from that of the bulk PDMS (50% C, 25% O, and 25% Si). At greater depths into the sample there was a sharp increase in the oxygen concentration (~50%) at 10 nm from the bottom surface (i.e., the surface that was exposed to the plasma), which is consistent with previous measurements of the surface following similar oxygen plasma treatment.[32] Figure 1c shows that the thickness and CA of the membrane were consistent for more than 10 transfer steps. The AFM image shown in Figure 1d indicates that the surface was relatively clean and smooth, with an average roughness of R_a < 6 nm, even after repeated transfers. In contrast to the PDMS oligomer, the transferred membranes exhibited constant hydrophobicity following washing with acetone, as shown in Figure 1e. Moreover, the properties of the siloxane chain and methyl group observed using Fourier transform infrared (FTIR) spectroscopy (see Supporting Information Figure S2) suggest that the membrane can be expected to be hydrophobic.

Figure 2 shows FTIR spectra of pristine PDMS, plasma treated PDMS, and heat and plasma treated PDMS. The most marked variation was 1018−1080 cm^{-1}, corresponding to the Si−O−Si chain, the peak at 1259 cm^{-1}, which corresponds to the symmetric methyl deformation of $Si-CH_3$, and the peak at 796 cm^{-1}, which corresponds to in-plane rocking vibration in $Si-CH_3$.[35,36]

Following plasma treatment, the chemical composition of the surface of the PDMS was converted to a silica-like (SiO_x) formation. The peaks at 1018−1080 cm^{-1} decreased in intensity because the number of asymmetric Si−O−Si bonds decreased.[37] The loss of methyl functional groups is consistent with the decrease in the intensity of the peaks at 1259 cm^{-1}. Following heat treatment, the intensity of the peak at 1018−1080 cm^{-1} corresponding to Si−O−Si bonds increased again, which is attributable to condensation of the unstable plasma-

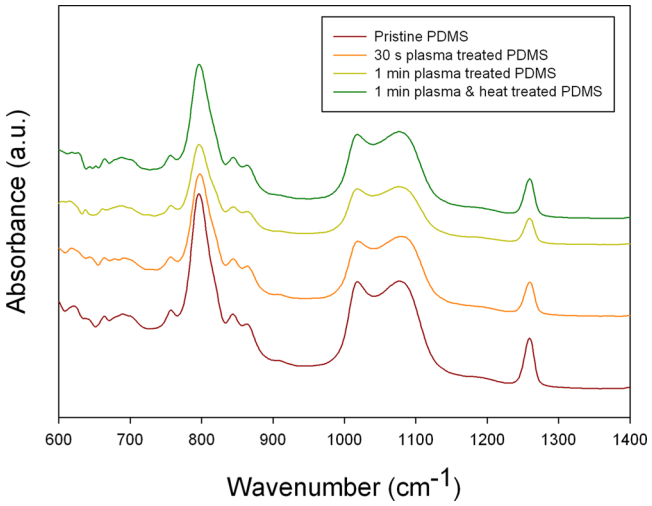

Figure 2. FTIR spectra results of pristine PDMS, 30 s plasma treated PDMS, 1 min plasma treated PDMS, and 1 min plasma/heat treated PDMS.

treated region.[38,39] This reaction transforms the plasma-treated layer into a well-defined thin membrane, which has mechanical properties different from those of the bulk PDMS, which enables repeatable membrane transfer.

The results of simulations (see Supporting Information Figure S3) show that the temperature profile extends for a few hundreds of micrometers into the bulk. It follows that, although heat penetrates much deeper than the chemical modifications due to the plasma treatment, significant effects occur only in the regions that have been affected by both the thermal and the plasma treatment processes. Further evidence for this is that there was no significant change in the thickness of the membrane as a function of the heating time (Supporting Information Figure S4). It follows that control over the thickness of the membranes can be achieved by varying the conditions in the plasma process.

Thickness of the Transferred Patterns Following Various Conditions. To determine the role of the oxygen plasma, we first investigated the thickness of oxidized layer using an 800 nm pitch line-and-space pattern with the height of 600 nm (see Supporting Information Figure S5). It is well-known that the oxygen diffusivity and plasma density affect the thickness of the modified region of PDMS;[40] therefore, the location of the cohesion failure is expected to be determined by the penetration depth of the plasma treatment. Figure 3a shows an atomic force microscope (AFM) image of a representative PDMS pattern following the pattern transfer process, demonstrating that the patterned surface was uniform over the large area, with a rounded surface profile. The height of the patterned features was in the range 125−330 nm, which is greater than that of the uniform membrane shown in Figure 1: this is attributed to enhanced oxidation via lateral diffusion of oxygen.

The thickness of transferred line patterns depended on the plasma treatment conditions, that is, the plasma power and exposure time. Figure 3b shows the results of pattern transfer with different plasma treatment conditions. The samples were cured for 1.5 h with a mixing ratio of 10:1. The average thickness of the patterns treated with a power of 18 W for 1 min was ∼340 nm. When a smaller power (7 W) was used, the average thickness reduced to ∼230 nm, and when a shorter exposure time (30 s) was used, the average height was ∼220 nm.

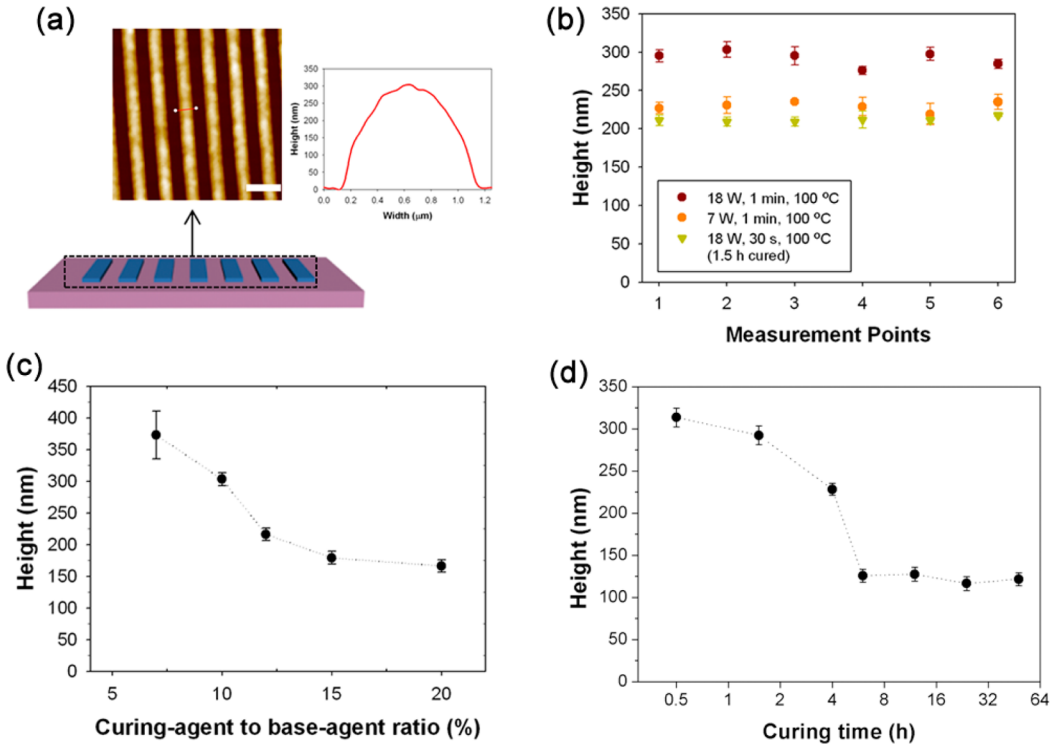

Figure 3. (a) Representative AFM image of transferred pattern along with its cross-sectional profile. Scale bar represents 2 μm. (b) Change of pattern height with various plasma treatment conditions. (c) Change of pattern height as a function of curing agent to base-agent ratio from 7% to 20%. (d) Change of pattern height as a function of curing time from 0.5 and 48 h.

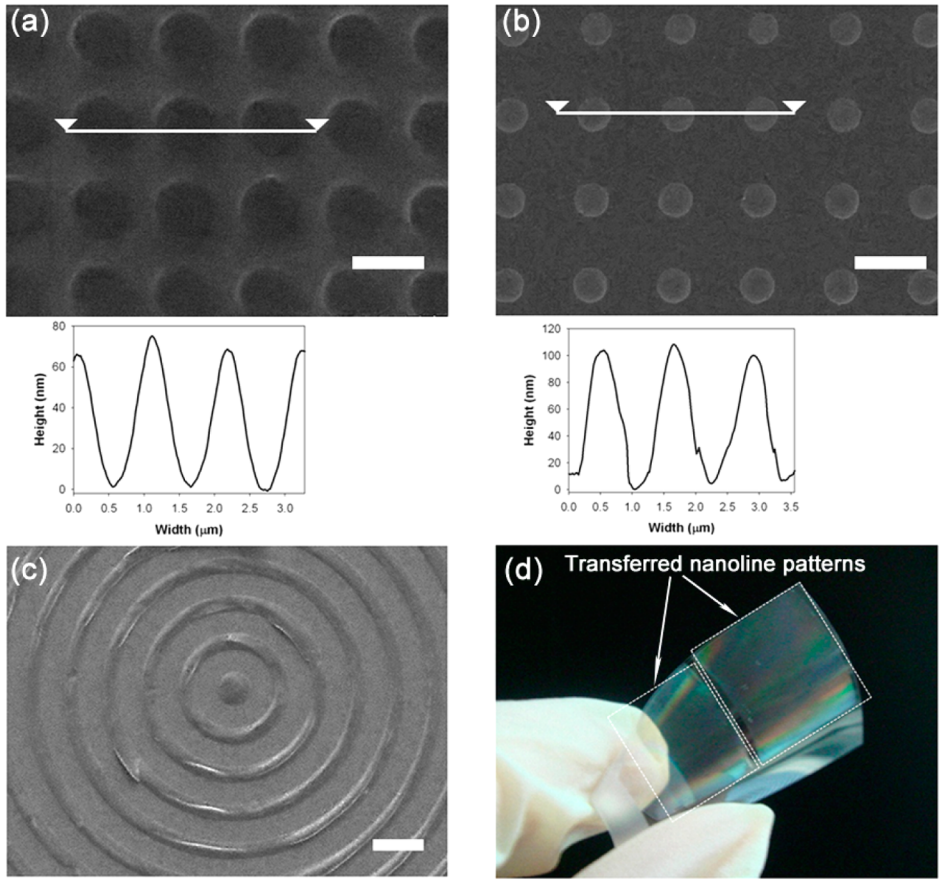

Figure 4. (a–c) SEM images for various transferred patterns: (a) PDMS membrane with holes, (b) PDMS dot arrays, and (c) large concentric circle patterns. Scale bars of (a), (b), and (c) represent 1 and 100 μm, respectively. (d) Large-area transferred PDMS line patterns on flexible PET film.

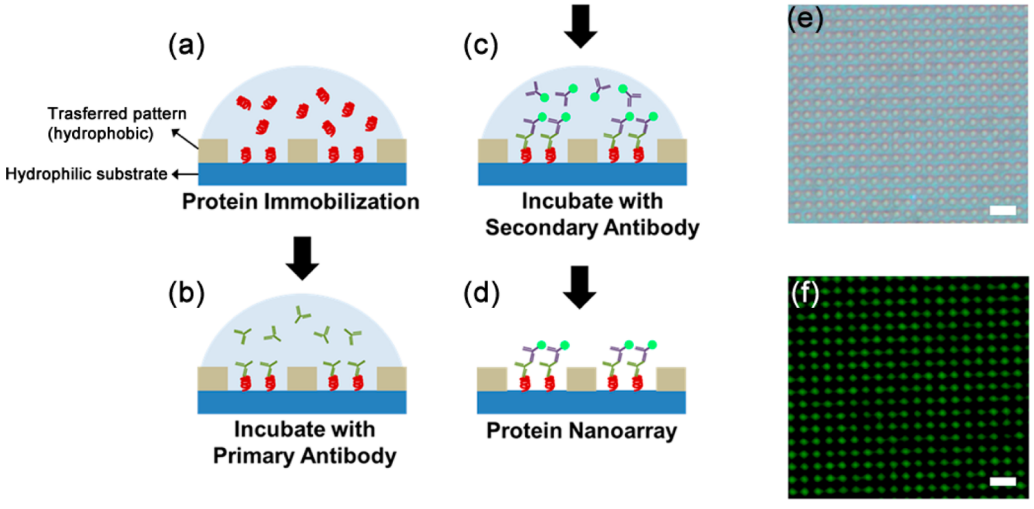

Figure 5. (a–d) Schematics of the protein immobilization and immunoassay. (e) The optical image of the transferred 800 nm nanowell pattern. (f) Fluorescence microscope image of the fluorescein isotiocyanate conjugated goat antirabbit IgG. Scale bars of (e) and (f) represent 3 μm.

In addition to the plasma treatment conditions, we were able to control the thickness of the oxidized layer by varying the diffusivity of oxygen plasma. The free volume of the polymers, which is related to the cross-linking density, affects the oxygen diffusivity, as well as the mechanical properties such as modulus,[25] storage of uncured molecules,[41] and permeability.[42] In addition, the curing conditions during cross-linking can modify these characteristics.[43] Hence, the depth of the PDMS skin layer could be controlled by varying the ratio of the curing agent to the base polymer, as shown in Figure 3c, in which the amount of curing agent was varied in the range 7–20%, indicating that the apparent oxygen diffusivity in the harder PDMS was less than that in the softer PDMS. It apperars that, under the current conditions, the penetration depth of the plasma was approximately equal to the height of the transferred pattern, which was in the range 160–340 nm.

Similarly, the variation in the thickness of the transferred patterns is shown in Figure 3d as a function of the curing time

(with fixed curing conditions and a mixing ratio of 10:1). A curing of 20 min resulted in a thickness of ~330 nm, which was decreased to ~125 nm following curing for 6 h. As the curing time increased further, the pattern thickness saturated at ~120 nm. Such saturation is consistent with the previous report by Schiabone et al.,[26] suggesting that the modulus is correlated with the thickness of the transferred pattern.

Shape Transfer and Applications. Figure 4 shows that various patterns can be formed on rigid and flexible substrates, including polyethylene terephthalate (PET), with the same process parameters. By coating of the surface with an adhesive primer that contains silane compounds, silanol groups can be formed following the oxygen plasma treatment. This surface treatment facilitates pattern transfer onto a flexible substrate.

One of the most important advantages of this approach is its generation of a residue-free pattern. Because the transferred pattern is hydrophobic, but the exposed silica surface was very hydrophilic, it is possible to create a protein array that was aligned to a tolerance of 800 nm. Figure 5 shows the wells patterned on the SiO_2 substrate. In general, proteins have higher affinity for polar surfaces, such as SiO_2, than nonpolar surface; thus proteins can be selectively immobilized on the exposed SiO_2 regions.[44,45]

Although there exist a number of methods to create protein arrays, including nanoimprint,[46] photo lithography,[47] and dip-pen lithography,[48] these methods are typically relatively expensive and require multiple process steps. Using the membrane transfer method described here, we fabricated submicrometer well structures on a glass substrate. The patterned substrate was covered with HFN solution at room temperature to achieve protein immobilization, and subsequently visualized through the specific antibody−antigen reaction between rabbit antifibronectic and fluorescein isothiocyanate (FITC) conjugated goat antirabbit IgG. Figure 5f shows the fluorescence image, revealing well-aligned protein arrays.

The transferred patterns act as a physically deposited hydrophobic self-assembled monolayer and do not require a mask or lift-off process. The process is therefore not only facile and low-cost but also biocompatible, and hence has potential applications in biosensors and observation of protein−cell interactions.

4. CONCLUSION

We have demonstrated controlled and repetitive transfer of thin PDMS membranes via CMF from bulk PDMS block on substrates including SiO_2 via oxygen plasma treatment and heating. The transferred membranes had a thickness in the range 60−80 nm and were hydrophobic. The thickness of the transferred membrane could be controlled by varying the cross-linking and plasma treatment conditions. These conditions determine the penetration of oxygen into the PDMS, and hence the range over which the mechanical properties were transformed, which determines the location of the interfacial fracture plane and therefore the thickness of the membrane. This method was used to fabricate residual-free patterns with controllable dimensions. This represents a facile and repeatable process to pattern surfaces with potential applications in areas of selective deposition of biological samples, such as cells, proteins, and DNA.

■ ASSOCIATED CONTENT

Ⓢ Supporting Information

Optical images, FTIR data of the transferred membrane, simulation result of heat transfer, and SEM image. This material is available free of charge via the Internet at http://pubs.acs.org.

■ AUTHOR INFORMATION

Corresponding Author

*E-mail: pkim@kaist.ac.kr.

Notes

The authors declare no competing financial interest.

■ ACKNOWLEDGMENTS

We gratefully acknowledge support from the National Global Frontier R&D Program on Center for Multiscale Energy System funded by the National Research Foundation under the Ministry of Science, ICT & Future Planning, Korea (2011-0031561, 2011-0031577), and MOTIE/KEIT Program (Grant 10045070). This work was also supported in part by the National Research Foundation of Korea (NRF-2011-35B-D00013).

■ REFERENCES

(1) Quake, S. R.; Scherer, A. From Micro- to Nanofabrication with Soft Materials. *Science* **2000**, *290*, 1536−1540.
(2) Hamley, I. W. Nanotechnology with Soft Materials. *Angew. Chem., Int. Ed.* **2003**, *42*, 1692−1712.
(3) Gates, B. D.; Xu, Q. B.; Love, J. C.; Wolfe, D. B.; Whitesides, G. M. Unconventional Nanofabrication. *Annu. Rev. Mater. Res.* **2004**, *34*, 339−372.
(4) Carrillo, F.; Gupta, S.; Balooch, M.; Marshall, S. J.; Marshall, G. W.; Pruitt, L.; Puttlitz, C. M. Nanoindentation of Polydimethylsiloxane Elastomers: Effect of Crosslinking, Work of Adhesion, and Fluid Environment on Elastic Modulus. *J. Mater. Res.* **2005**, *20*, 2820−2830.
(5) Varga, Z.; Filipcsei, G.; Zrinyi, M. Magnetic Field Sensitive Functional Elastomers with Tuneable Elastic Modulus. *Polymer* **2006**, *47*, 227−233.
(6) Fukushima, T.; Kosaka, A.; Yamamoto, Y.; Aimiya, T.; Notazawa, S.; Takigawa, T.; Inabe, T.; Aida, T. Dramatic Effect of Dispersed Carbon Nanotubes on the Mechanical and Electroconductive Properties of Polymers Derived from Ionic Liquids. *Small* **2006**, *2*, 554−560.
(7) Kofod, G.; Risse, S.; Stoyanov, H.; McCarthy, D. N.; Sokolov, S.; Kraehnert, R. Broad-Spectrum Enhancement of Polymer Composite Dielectric Constant at Ultra Low Volume Fractions of Silica-Supported Copper Nanoparticles. *ACS Nano* **2011**, *5*, 1623−1629.
(8) Huck, W. T. S. Artificial Skins - Hierarchical Wrinkling. *Nat. Mater.* **2005**, *4*, 271−272.
(9) Greene, G.; Yao, G.; Tannenbaum, R. Deposition and Wetting Characteristics of Polyelectrolyte Multilayers on Plasma-Modified Porous Polyethylene. *Langmuir* **2004**, *20*, 2739−2745.
(10) Zhang, Y.; Reed, J. C.; Yang, S. Creating a Library of Complex Metallic Nanostructures Via Harnessing Pattern Transformation of a Single Pdms Membrane. *ACS Nano* **2009**, *3*, 2412−2418.
(11) Huntington, M. D.; Engel, C. J.; Hryn, A. J.; Odom, T. W. Polymer Nanowrinkles with Continuously Tunable Wavelengths. *ACS Appl. Mater. Interfaces* **2013**, *5*, 6438−6442.
(12) Fabregat, G.; Cordova-Mateo, E.; Armelin, E.; Bertran, O.; Aleman, C. Ultrathin Films of Polypyrrole Derivatives for Dopamine Detection. *J. Phys. Chem. C* **2011**, *115*, 14933−14941.
(13) Ferreira, C. A.; Casanovas, J.; Rodrigues, M. A. S.; Muller, F.; Armelin, E.; Aleman, C. Transport of Metallic Ions through Polyaniline-Containing Composite Membranes. *J. Chem. Eng. Data* **2010**, *55*, 4801−4807.

(14) Watanabe, H.; Fujimoto, A.; Takahara, A. Manipulation of Surface Properties: The Use of Nanomembrane as a Nanometre-Thick Decal. *Soft Matter* **2011**, *7*, 1856−1860.
(15) Watanabe, H.; Fujimoto, A.; Takahara, A. Concealing Surface Topography by Attachment of Nanometer-Thick Film. *Langmuir* **2013**, *29*, 2906−2911.
(16) Wong, M.; Ishige, R.; White, K. L.; Li, P.; Kim, D.; Krishnamoorti, R.; Gunther, R.; Higuchi, T.; Jinnai, H.; Takahara, A.; Nishimura, R.; Sue, H. J. Large-Scale Self-Assembled Zirconium Phosphate Smectic Layers Via a Simple Spray-Coating Process. *Nat. Commun.* **2014**, *5*, 3589.
(17) Olah, A.; Hillborg, H.; Vancso, G. J. Hydrophobic Recovery of Uv/Ozone Treated Poly(Dimethylsiloxane): Adhesion Studies by Contact Mechanics and Mechanism of Surface Modification. *Appl. Surf. Sci.* **2005**, *239*, 410−423.
(18) Sanii, B.; Parikh, A. N. Patterning Fluid and Elastomeric Surfaces Using Short-Wavelength Uv Radiation and Photogenerated Reactive Oxygen Species. *Annu. Rev. Phys. Chem.* **2008**, *59*, 411−432.
(19) Zheng, Z. J.; Azzaroni, O.; Zhou, F.; Huck, W. T. S. Topography Printing to Locally Control Wettability. *J. Am. Chem. Soc.* **2006**, *128*, 7730−7731.
(20) Kim, P.; Kwak, R.; Lee, S. H.; Suh, K. Y. Solvent-Assisted Decal Transfer Lithography by Oxygen-Plasma Bonding and Anisotropic Swelling. *Adv. Mater.* **2010**, *22*, 2426−+.
(21) Kim, Y. K.; Kim, G. T.; Ha, J. S. Simple Patterning Via Adhesion between a Buffered-Oxide Etchant-Treated Pdms Stamp and a Sio2 Substrate. *Adv. Funct. Mater.* **2007**, *17*, 2125−2132.
(22) Thangawng, A. L.; Swartz, M. A.; Glucksberg, M. R.; Ruoff, R. S. Bond-Detach Lithography: A Method for Micro/Nanolithography by Precision Pdms Patterning. *Small* **2007**, *3*, 132−138.
(23) Childs, W. R.; Nuzzo, R. G. Large-Area Patterning of Coinage-Metal Thin Films Using Decal Transfer Lithography. *Langmuir* **2005**, *21*, 195−202.
(24) Park, J. Y.; Yoo, S. J.; Lee, E. J.; Lee, D. H.; Kim, J. Y.; Lee, S. H. Increased Poly(Dimethylsiloxane) Stiffness Improves Viability and Morphology of Mouse Fibroblast Cells. *Biochip J.* **2010**, *4*, 230−236.
(25) Nguyen, Q. T.; Bendjama, Z.; Clement, R.; Ping, Z. H. Poly(Dimethylsiloxane) Crosslinked in Different Conditions Part I. Sorption Properties in Water-Ethyl Acetate Mixtures. *Phys. Chem. Chem. Phys.* **1999**, *1*, 2761−2766.
(26) Fuard, D.; Tzvetkova-Chevolleau, T.; Decossas, S.; Tracqui, P.; Schiavone, P. Optimization of Poly-Di-Methyl-Siloxane (PDMS) Substrates for Studying Cellular Adhesion and Motility. *Microelectron. Eng.* **2008**, *85*, 1289−1293.
(27) Amirsadeghi, A.; Lee, J. J.; Park, S. A Simulation Study on the Effect of Cross-Linking Agent Concentration for Defect Tolerant Demolding in Uv Nanoimprint Lithography. *Langmuir* **2012**, *28*, 11546−11554.
(28) Takahiro, S. *Fracture Nanomechanics*; Pan Stanford Publications: Singapore, 2011; Chapter 5, pp 134−173.
(29) Childs, W. R.; Nuzzo, R. G. Decal Transfer Microlithography: A New Soft-Lithographic Patterning Method. *J. Am. Chem. Soc.* **2002**, *124*, 13583−13596.
(30) Hillborg, H.; Ankner, J. F.; Gedde, U. W.; Smith, G. D.; Yasuda, H. K.; Wikstrom, K. Crosslinked Polydimethylsiloxane Exposed to Oxygen Plasma Studied by Neutron Reflectometry and Other Surface Specific Techniques. *Polymer* **2000**, *41*, 6851−6863.
(31) Suni, T.; Henttinen, K.; Suni, I.; Makinen, J. Effects of Plasma Activation on Hydrophilic Bonding of Si and Sio2. *J. Electrochem. Soc.* **2002**, *149*, G348−G351.
(32) Park, J. Y.; Chae, H. Y.; Chung, C. H.; Sim, S. J.; Park, J.; Lee, H. H.; Yoo, P. J. Controlled Wavelength Reduction in Surface Wrinkling of Poly(Dimethylsiloxane). *Soft Matter* **2010**, *6*, 677−684.
(33) Pretzl, M.; Schweikart, A.; Hanske, C.; Chiche, A.; Zettl, U.; Horn, A.; Boker, A.; Fery, A. A Lithography-Free Pathway for Chemical Microstructuring of Macromolecules from Aqueous Solution Based on Wrinkling. *Langmuir* **2008**, *24*, 12748−12753.
(34) Volinsky, A. A.; Moody, N. R.; Gerberich, W. W. Interfacial Toughness Measurements for Thin Films on Substrates. *Acta Mater.* **2002**, *50*, 441−466.
(35) Efimenko, K.; Wallace, W. E.; Genzer, J. Surface Modification of Sylgard-184 Poly(Dimethyl Siloxane) Networks by Ultraviolet and Ultraviolet/Ozone Treatment. *J. Colloid Interface Sci.* **2002**, *254*, 306−315.
(36) Bodas, D.; Khan-Malek, C. Formation of More Stable Hydrophilic Surfaces of Pdms by Plasma and Chemical Treatments. *Microelectron. Eng.* **2006**, *83*, 1277−1279.
(37) Lycans, R. M.; Higgins, C. B.; Tanner, M. S.; Blough, E. R.; Day, B. S. Plasma Treatment of Pdms for Applications of in Vitro Motility Assays. *Colloids Surf., B* **2014**, *116*, 687−694.
(38) Abdelmouleh, M.; Boufi, S.; Belgacem, M. N.; Duarte, A. P.; Ben Salah, A.; Gandini, A. Modification of Cellulosic Fibres with Functionalised Silanes: Development of Surface Properties. *Int. J. Adhes. Adhes.* **2004**, *24*, 43−54.
(39) Yoo, J. J.; Rhee, S. H. Evaluations of Bioactivity and Mechanical Properties of Poly (Epsilon-Caprolactone) Silica Nanocomposite Following Heat Treatment. *J. Biomed Mater. Res., Part A* **2004**, *68A*, 401−410.
(40) Shi, H.; H, H.; Bao, J.; Im, J.; Ho, P. S.; Zhou, Y.; Pender, J. T.; Armacost, M.; Kyser, D. Plasma Altered Layer Model for Plasma Damage Characterization of Porous Osg Films. *Proc. IEEE Int. Interconnect Technol. Conf.* **2009**, 78−80.
(41) Lee, J. H.; Lee, Y. M.; Kim, Y. H.; Lee, J. Y.; Choi, S. J.; Yoo, P. J. Liquid-Liquid Interfacial Nanomolding. *Small* **2011**, *7*, 2587−2592.
(42) Shantarovich, V. P.; Kevdina, I. B.; Yampolskii, Y. P.; Alentiev, A. Y. Positron Annihilation Lifetime Study of High and Low Free Volume Glassy Polymers: Effects of Free Volume Sizes on the Permeability and Permselectivity. *Macromolecules* **2000**, *33*, 7453−7466.
(43) Ding, Y. Z.; Garland, S.; Howland, M.; Revzin, A.; Pan, T. R. Universal Nanopatternable Interfacial Bonding. *Adv. Mater.* **2011**, *23*, 5551.
(44) Altankov, G.; Groth, T.; Krasteva, N.; Albrecht, W.; Paul, D. Morphological Evidence for a Different Fibronectin Receptor Organization and Function During Fibroblast Adhesion on Hydrophilic and Hydrophobic Glass Substrata. *J. Biomater. Sci., Polym. Ed.* **1997**, *8*, 721−740.
(45) Lee, H. U.; Park, S. Y.; Kang, Y. H.; Jeong, S. Y.; Choi, S. H.; Jahng, K. Y.; Cho, C. R. Surface Modification of and Selective Protein Attachment to a Flexible Microarray Pattern Using Atmospheric Plasma with a Reactive Gas. *Acta Biomater.* **2010**, *6*, 519−525.
(46) Hoff, J. D.; Cheng, L. J.; Meyhofer, E.; Guo, L. J.; Hunt, A. J. Nanoscale Protein Patterning by Imprint Lithography. *Nano Lett.* **2004**, *4*, 853−857.
(47) Senaratne, W.; Sengupta, P.; Jakubek, V.; Holowka, D.; Ober, C. K.; Baird, B. Functionalized Surface Arrays for Spatial Targeting of Immune Cell Signaling. *J. Am. Chem. Soc.* **2006**, *128*, 5594−5595.
(48) Demers, L. M.; Ginger, D. S.; Park, S. J.; Li, Z.; Chung, S. W.; Mirkin, C. A. Direct Patterning of Modified Oligonucleotides on Metals and Insulators by Dip-Pen Nanolithography. *Science* **2002**, *296*, 1836−1838.